

Active control of transport through nanopores

Cheng Lian^{1,2} and Wei Zhong^{3,4, a)}

¹⁾State Key Laboratory of Chemical Engineering, Shanghai Engineering Research Center of Hierarchical Nanomaterials, and School of Chemistry and Molecular Engineering, East China University of Science and Technology, Shanghai 200237, P. R. China.

²⁾Institute for Theoretical Physics, Utrecht University, Princetonplein 5, 3584 CC Utrecht, The Netherlands.

³⁾Minjiang Collaborative Center for Theoretical Physics, College of Physics and Electronic Information Engineering, Minjiang University, Fuzhou 350108, P. R. China.

⁴⁾Department of Information and Computing Sciences, Utrecht University, Princetonplein 5, 3584 CC Utrecht, The Netherlands.

(Dated: 21 July 2021)

Passive particle transport through narrow channels is well studied, while for active particle system, it is not well understood. Here, we demonstrate the active control of the transport through a nanopore via mean-field analysis and molecular dynamics simulations. We prove that the active force enhances the transport efficiency with an effective diffusion coefficient $D_{\text{eff}} = D_t(1 + Pe^2/6)$, where D_t is the translational diffusion coefficient, and Pe is the Péclet number that determines the strength of the active force. For the number of particles inside the channel, it experiences subdiffusion at short times and then turns to normal at longer times. Finally, we extend our research for several sinusoidal shapes of the channel surface. More particles are trapped in the channel if the roughness of the channel surface is increased, resulting in fewer particles are transported from one side of the channel to the other.

I. INTRODUCTION

The transport of molecules through a micro- or nanopore plays a vital role in many biological and chemical systems¹. The translocation dynamics of DNA, protein and ions through cell membrane are still an ongoing field^{2,3}, different methods have been used to understand and control those transport processes⁴⁻⁸. Normally, an external field is required to activate and speed up the transport, where the external field can be pressure, temperature or potential differences^{1,9}. However, there is a large group of microorganisms, known as active matter, that makes the external field no longer the only driven source during the transport process.

Active matter, known as the microswimmers or active Brownian particles (ABPs), can convert the energy from the environment into its own self-propelled velocity¹⁰⁻¹². Recently, active matter attracts a lot of attention. After the first well-known model to describe the flocking of the birds, i.e., the Vicsek model¹³, the field of active matter receives a number of important progresses. One of the most impressive progress is the motility-induced phase separation (MIPS)¹⁴⁻¹⁶, which helps us understand the phase behavior of the ABPs, although the universality class at its critical point is still

under debate^{17,18}. Besides, many researchers study the dense phase of the ABPs, with the glass transition and hexatic phase¹⁹⁻²⁴. However, in real experiments, it is hard to squeeze the active particle into very dense phase, the mixture of the active and passive particles brings a possible solution²⁵⁻²⁷.

Most studies about active matter focus on the bulk properties, obtained under periodic boundary conditions, few has paid attention to the transports of active matter under confinement. The active particles can be trapped or sorted by the solid boundary, the concentration gradient, or the obstacles²⁸⁻³¹, and the motion of the active particles can be rectified by a pattern microchannel³². When active particles are moving inside a channel³³⁻³⁶, it was found that the weak external field has strong influence on velocity profiles and particle flow. Even though the transport dynamics of the active Brownian particles passing through a nanopore is not well understood.

In this paper, we use molecular dynamics (MD) simulations to investigate the transport dynamics of the active Brownian particles passing through a nanopore. We first demonstrate the mean-field analysis of the transport dynamics, revealing that for large self-propelled speed, the active force accelerates the transport with an effective diffusion coefficient $D_{\text{eff}} = D_t(1 + Pe^2/6)$, where D_t is the translational diffusion coefficient, and Pe is the Péclet number that determines the strength of the active force. Then we compare our

^{a)}Electronic mail: zhongwei2284@hotmail.com.

MD results to the mean-field analytical solution, it is found that they are consistent. The mean-square displacement (MSD) of the particle number in the channel is also obtained, indicating that the diffusion of particle in the channel follows anomalous diffusion at short times, then turn to normal diffusion at long times. Finally, the effect of the channel surface roughness on the transport is studied. In contrast with the straight channel, more particles are willing to stay in the channel if the roughness increases, resulting in slower passing through dynamics of the active particles.

II. OVERDAMPED ACTIVE BROWNIAN PARTICLES

We consider a two dimensional (2D) system with two rectangle chambers A and C (As shown in Fig. 1), whose sizes are $L_x = 50\sigma$ and $L_y = 20\sigma$, connected by a narrow channel B of length $l = 10\sigma$ and width $d = 3\sigma$, where σ is the nominal particle diameter. The boundary is built by the active Brownian particles with fixed position.

The particles in the system interact with each other via the Weeks-Chandler-Anderson (WCA) potential, i.e., $U(r) = 4\epsilon[(\sigma/r)^{12} - (\sigma/r)^6] + \epsilon$ if $r \leq 2^{1/6}$, and zero otherwise. Here, ϵ represents the interaction strength, and r is the center-to-center distance between two particles. We use $\epsilon = 1/\beta = k_B T$ during our simulation, where β is the inverse thermal energy, k_B is the Boltzmann constant, and T is the temperature of the system. The model can be described as the overdamped Langevin equation³⁷⁻³⁹,

$$\begin{aligned} \dot{\mathbf{r}}_i &= D_t \beta [\mathbf{F}_i + F_p \hat{\mathbf{v}}_i] + \sqrt{2D_t} \boldsymbol{\eta}_i \\ \dot{\theta}_i &= \sqrt{2D_r} \eta_r \end{aligned} \quad (1)$$

where $\mathbf{r}_i(t)$ and $\theta_i(t)$ are the position and orientation of the i th particle at time t . \mathbf{F}_i is the total excluded-volume repulsive force on the i th particle, which is given by the WCA potential. F_p is a constant self-propulsion force on particle i , and the direction function $\hat{\mathbf{v}}_i = (\cos(\theta_i), \sin(\theta_i))$. D_t and $D_r = 3D_t/\sigma^2$ represent the translational and rotational diffusion coefficient, respectively. The translational and the rotational time scales are $\tau_t = \sigma^2/2D_t$ and $\tau_r = 1/2D_r$. η_t and η_r are two Gaussian white noise terms with $\langle \eta_t \rangle = 0$, $\langle \eta_r \rangle = 0$ and $\langle \eta_t(t) \eta_t(t') \rangle = 2D_t \delta(t - t')$, $\langle \eta_r(t) \eta_r(t') \rangle = 2D_r \delta(t - t')$. The Péclet number, defined as the ratio of advective and diffusive transport rates, is defined as $Pe = v_p \tau_t / \sigma$, where $v_p = D_t \beta F_p$ is the self-propelled speed of an individual particle.

At the beginning of the molecular dynamics (MD) simulations, we place N particles uniformly distributed in the top chamber (Fig.1), then evolve the system. At each time, we measure the numbers of particles in different regions, i.e., N_A , N_B , and N_C are the particle numbers in the top chamber, channel, and bottom chamber, respectively. The total number of the particles is $N \equiv N_A + N_B + N_C$.

The molecular dynamics (MD) simulations used here are coded in *c programming* and the time unit used here refer to one move per particle within a short time $dt = 0.00001$. Running about 25 independent samples provide us with fairly accurate values of the particle numbers in different position and time.

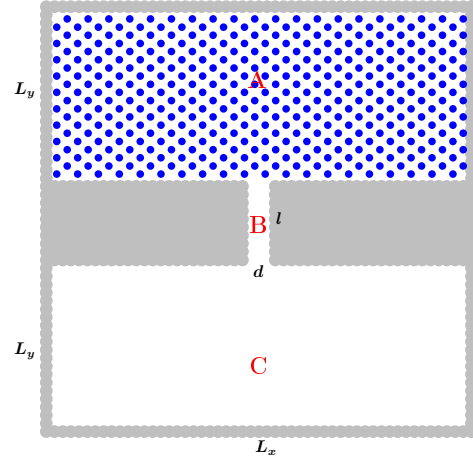


FIG. 1. The schematic diagram of the 2D system. Two rectangle chambers, with their sizes $L_x = 50\sigma$ and $L_y = 20\sigma$, are connected by a narrow channel of length $l = 10\sigma$ and width $d = 3\sigma$. All active particles are placed uniformly in the upper chamber at $t = 0$.

III. NANO-SCALE TRANSPORT OF ABPS

A. Mean-field theory understanding

Supposing we set a uniform distribution of the initial angles $\theta(0) = 0$, the mean-square displacement from the initial position $r(0)$ evolves as^{40,44}

$$\begin{aligned} \langle [r(t) - r(0)]^2 \rangle &= 4D_t t + \frac{v_p^2 \tau_r^2}{2} \left[\frac{2t}{\tau_r} + e^{-2t/\tau_r} - 1 \right] \\ &\approx 4D_{\text{eff}} t. \end{aligned} \quad (2)$$

When $t \gg \tau_r$, the effective diffusion coefficient is expressed as

$$\begin{aligned} D_{\text{eff}} &= D_t + \frac{v_p^2 \tau_r}{4} \\ &= D_t \left(1 + Pe^2 \frac{D_t}{2\sigma^2 D_r} \right) \\ &= D_t \left(1 + \frac{Pe^2}{6} \right). \end{aligned} \quad (3)$$

The diffusion equation for the density of active Brownian particles $c(y, t)$ can be written as

$$\partial_t c(y, t) = \partial_y D_{\text{eff}} \partial_y c(y, t), \quad (4)$$

Base on the analytic solution of Eq. 4 from refs.^{45,46} and the similar behavior found in the ions transport in supercapacitors⁴¹⁻⁴³, one finds that the particle number $N - N_A$ increases linearly in time at early times:

$$N - N_A \sim t \quad (5)$$

Then it experiences a square-root behaviour with a short time range, i.e.,

$$N - N_A \sim \sqrt{D_{\text{eff}} t}. \quad (6)$$

Finally, $N - N_A$ increases exponentially in time as

$$N - N_A \sim 1 - \exp(-\sqrt{D_{\text{eff}} t}/\tau). \quad (7)$$

where τ is a constant.

The mean-field analysis indicates that the active force accelerates the transport with a prefactor linear in $\sqrt{D_{\text{eff}}}$.

B. Dynamics from MD simulations

As discussed through the mean-field analysis, we expect that the active force will accelerate the transport dynamics. In order to determine the acceleration of the dynamics by the active force numerically, two different sets of simulations have been performed using the MD algorithm. In the first set, the Péclet number is fixed at $Pe = 200$. Since we only focus on dilute situation, the initial number of particles on the top chamber is set to be $N = 400, 225, \text{ and } 100$. In the other set, under the constrain that the number of particles is $N = 400$, three different Péclet numbers $Pe = 50, 100 \text{ and } 200$ are employed during the simulations.

The results shown in Fig. 2(a) suggest that indeed the active force accelerates the dynamics with a prefactor linear in $\sqrt{D_{\text{eff}}}$, i.e., $(N - N_A)/N \sim f(t\sqrt{D_{\text{eff}}})$.

After a noisy initial part, $N - N_A$ increases linear in time. Then it turn to a square-root growth for a short time range. For longer times, $N - N_A \sim 1 - \exp(-\sqrt{D_{\text{eff}} t}/\tau)$. These results are in agreement with the mean-field analysis (Eq. (5) - (7)).

The snapshots for different stages give more details about the transport process:

Very early stage I: As shown in fig.2 (b) I, at the beginning of the simulation, the particles are exploring the top chamber and the channel, none of them moved to the bottom chamber yet.

Linear regime II: After stage I, some of the particles begin to reach the bottom chamber. However, they still do not feel the spatial confinement of the bottom chamber, therefore particles are continuously entering into the bottom chamber, i.e., $N - N_A \sim t$.

Square-root diffusive regime III: As more particles enter into the bottom chamber, the spatial confinement becomes important, which slows down the particles moving from top chamber to bottom chamber, resulting in $N - N_A \sim \sqrt{t}$.

Exponential regime IV: Finally, the competition of the numbers of particles in both chambers indicates $N - N_A$ increases exponentially.

C. Dynamcis of the in-pore particles

To understand the dynamics of the particles in the channel, we define the mean-square deviation (MSD) of the in-pore particle number N_B as

$$\langle \Delta N_B(t)^2 \rangle = \langle [N_B(t) - N_B(0)]^2 \rangle \quad (8)$$

In our MD simulations, when the system reaches its steady state, we generate a long enough time series of $N_B(t)$, from which we calculate the MSD of N_B .

As shown in Fig. 3 that the MSD of N_B behaviors as $\langle \Delta N_B(t)^2 \rangle \sqrt{D_{\text{eff}}} \sim f(tD_{\text{eff}})$. At short times ($t \lesssim 10^5 / D_{\text{eff}}$), $\langle \Delta N_B(t)^2 \rangle \sim t^{0.5}$, which is a regime that the behavior of $\langle \Delta N_B(t)^2 \rangle$ is independent of the active force and it is identical to the diffusion of particles in the single-file^{47,48}. After that the number of particles in the channel diffuse normally.

In summary, for most existed systems, an external field is necessary to drive the particles to pass through the narrow channel. However, in nature, especially in many biological systems, some of the particles or microorganisms have a self-propelled force, and for those kind of systems, the active force itself dramatically improves the efficiency for particles to pass through a narrow channel. As we can see from both the mean-field

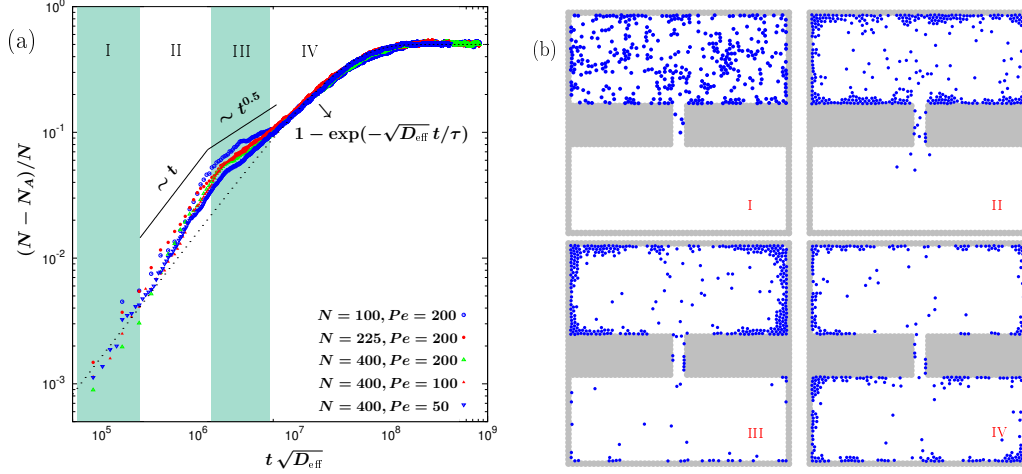


FIG. 2. (a) Dynamics of the particle number $N - N_A$ for different N and Pe . At very early times, particles are still exploring the area A and B . Then some of the particles begin to escape from the channel and move to C . However, they do not feel the space confinement of C , indicates that $N - N_A$ is linear in time. At the intermediate times, the space confinement in C slows down the speed for a particle passing from A to C . At this stage, $N - N_A \sim t^{0.5}$. Finally, particle number in A and C are near the steady-state, their behavior becomes exponential. (b) Typical snapshots for different time periods.

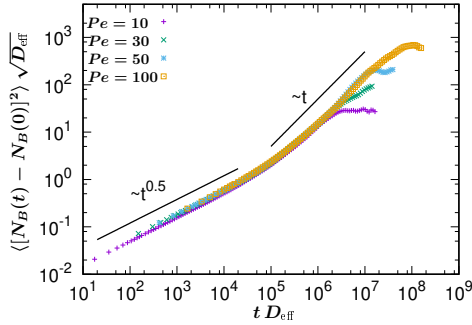


FIG. 3. The mean-square deviation of the particle number in the channel $\langle \Delta N_B(t)^2 \rangle$ for different Pe . For $t D_{\text{eff}} < 10^5$, it goes as $\langle \Delta N_B(t)^2 \rangle \sim t^{0.5}$. After that, $\langle \Delta N_B(t)^2 \rangle \sim \sqrt{D_{\text{eff}}} t$.

and simulation results that the active force enhances the transport with an effective diffusion coefficient D_{eff} . Besides, the number of particles inside the channel experiences anomalous diffusion at short times.

IV. AFFECTING TRANSPORT BY CHANNEL ROUGHNESS

In the previous section, we only focus on the straight channel. However, in most situations, the shape of the channel is not necessary to be straight. Here, the shape

of the channel is modified as

$$W(y) = \alpha \sin \left[\lambda \frac{y - (L_y + 1)\sigma}{\pi} \right] \quad \text{for } L_y \leq y < L_y + l, \quad (9)$$

where α is set to be unity, and λ is a roughness parameter. When λ is not equal to zero, it changes the roughness of the channel surface.

Three different λ (with $\lambda = 1, 3$ and 5) are considered. The particles are more willing to stay in the corner, therefore if we increase the roughness of the channel, more particles will be trapped in the channel (See TABLE I and Fig.4 (e) for more details.) and the speed for particles to move to the bottom chamber decreases.

Fig. 4(d) shows that for different roughness, the dynamics of $N - N_A$ is not affected dramatically. However, Fig. 4(e) confirms that more particles stay in the channel by increasing the roughness, leading to less number of particles move to the bottom chamber than the straight channel situation (As shown in Fig. 4(f)).

V. CONCLUSION

In this paper, we consider a two dimensional (2D) system with two rectangle chambers connected with a narrow channel. We distribute a few hundred of overdamped active Brownian particles in the top chamber, then evolve the system.

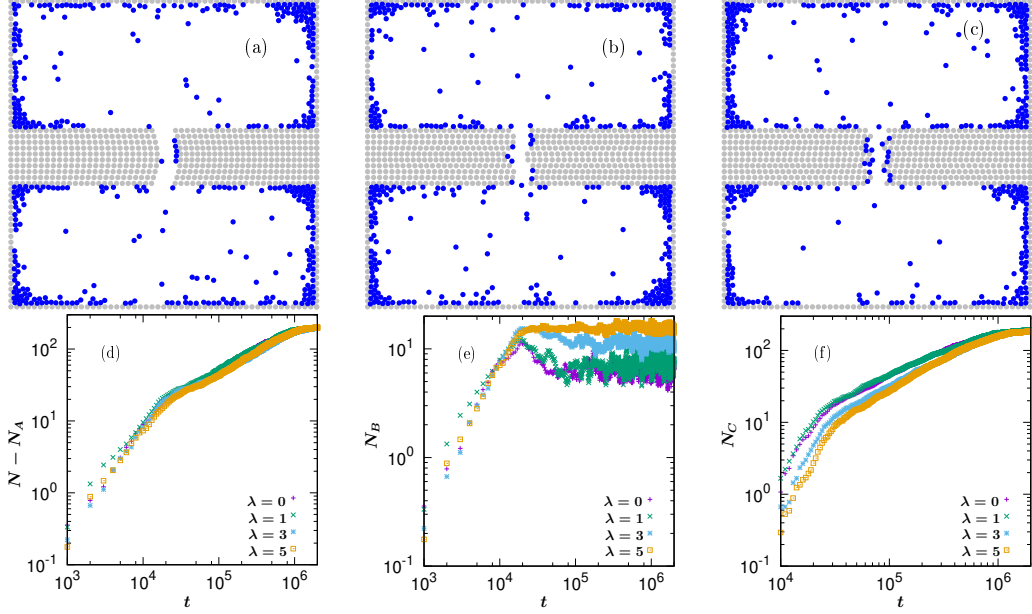


FIG. 4. (a)-(c) Snapshots when systems reach the steady-state for different roughness. Here $Pe = 200$, and the shape of the channel is expressed as $\alpha \sin(\lambda(y - L_y)/\pi)$, with $\alpha = 1$ and $\lambda = 1, 3, 5$ for (a)-(c), and when $\lambda = 0$, the channel is a straight channel as discussed in the previous section. (d)-(f) The effect of the roughness on the transport dynamics of the active Brownian particles passing through the narrow channel. The influence of the roughness to the number of particles left the top chamber is tiny, however, more particles would like to stay in the channel because of the roughness, so that the speed for particles go to the bottom chamber is decreasing.

t	5000	10000	50000	100000	500000	1000000
$N_B(\lambda = 0)$	0.92(2)	1.92(1)	1.96(2)	1.52(2)	1.80(2)	1.38(3)
$N_B(\lambda = 1)$	2.12(6)	7.88(6)	8.44(10)	7.22(12)	6.00(12)	8.00(10)
$N_B(\lambda = 3)$	3.00(10)	7.44(12)	13.22(8)	11.00(8)	11.22(6)	10.44(8)
$N_B(\lambda = 5)$	2.82(5)	7.05(6)	15.23(4)	15.52(4)	14.70(6)	15.17(3)

TABLE I. The average values of the number of active particles moving within the channel, i.e., N_B , at some particular time for different roughness parameters $\lambda = 0, 1, 3, 5$. Here, the Péclet number is set to be $Pe = 200$, the pore length and size are $l = 10\sigma$ and $d = 4\sigma$. At the initial time, 400 active particles are uniformly distributed on the top chamber.

By using the mean-field analysis and MD simulations, we find that the number of particles $N - N_A$ goes as $(N - N_A)/N \sim f(t\sqrt{D_{\text{eff}}})$. At short times, $N - N_A$ increases linear in time. Then after a slower dynamics regime, i.e., $N - N_A \sim \sqrt{t}$, the dynamics become exponential. In the meanwhile, at short times, the number of the particles in the channel experience anomalous diffusion $\langle \Delta N_B(t)^2 \rangle \sim \sqrt{t}$, then turn to normal diffusion at $t \gtrsim 10^6/D_{\text{eff}}$.

Finally, we change the roughness of the channel to be a *sinusoidal* shape. It is found that the straight channel is the most effective shape for active particles to pass through. Since active force is ubiquitous in many biological systems, when we try to understand the mechanism for microorganisms passing through a

nanopore, the effect from the active force should be considered.

ACKNOWLEDGEMENT

This research was sponsored by the EU-FET project NANOPHLOW (REP-766972-1), the National Natural Science Foundation of China (Nos. 91834301 and 22078088), and Shanghai Rising-Star Program (21QA1401900). The authors would like to thank Y. K. Zhu for his help in some simulations. We kindly thank J. de Graaf, R. van Roij, G. T. Barkema, and P. Huang for helpful discussions.

DATA AVAILABILITY

The data that support the findings of this study are available from the corresponding author upon reasonable request.

REFERENCES AND NOTES

- ¹M. Tagliazucchi and I. Szleifer, "Transport mechanisms in nanopores and nanochannels: can we mimic nature?" *Materials Today*, **18**, 131 (2015).
- ²J. Larkin *et al.* "Slow DNA transport through nanopores in hafnium oxide membranes," *ACS Nano* **7**, 10121 (2013).
- ³A. Meller and D. Branton, "Single molecule measurements of DNA transport through a nanopore," *Electrophoresis* **23**, 2583 (2002).
- ⁴U. F. Keyser, "Controlling molecular transport through nanopores," *J. R. Soc. Interface* **8**, 1369 (2011).
- ⁵E. Mádai *et al.* "Controlling ion transport through nanopores: modeling transistor behavior," *Phys. Chem. Chem. Phys.*, **20**, 24156 (2018).
- ⁶J. Dzubiella, R. J. Allen, and J.-P. Hansen, "Electric field-controlled water permeation coupled to ion transport through a nanopore," *J. Chem. Phys.* **120**, 5001 (2004).
- ⁷K. Misiunas and Ulrich F. Keyse, "Density-Dependent Speed-up of Particle Transport in Channels," *Phys. Rev. Lett.* **122**, 214501 (2019).
- ⁸H. L. Tao, C. Lian, and H. L. Liu, "Multiscale modeling of electrolytes in porous electrode: From equilibrium structure to non-equilibrium transport," *Green Energy & Environment* **5**, 303 (2020).
- ⁹M. Shankla and A. Aksimentiev, "Modulation of molecular flux using a graphene nanopore capacitor," *J. Phys. Chem. B* **121**, 3724 (2017).
- ¹⁰P. Romanczuk, *et al.* "Active Brownian particles," *Eur. Phys. J. Spec. Top.* **202**, 1 (2012).
- ¹¹C. Bechinger, *et al.*, "Active particles in complex and crowded environments," *Rev. Mod. Phys.* **88**, 045006 (2016).
- ¹²S. Ramaswamy, "Active matter," *J. Stat. Mech.* **054002** (2017).
- ¹³T. Vicsek *et al.* "Novel type of phase transition in a system of self-driven particles," *Phys. Rev. Lett.* **75**, 1226 (1995).
- ¹⁴J. Stenhammar, D. Marenduzzo, R. J. Allen and M. E. Cates, "Phase behaviour of active Brownian particles: the role of dimensionality," *Soft Matter*, **10**, 1489 (2014).
- ¹⁵M. E. Cates and J. Tailleur, "Motility-induced phase separation," *Annu. Rev. Condens. Matter Phys.* **6**, 219 (2015).
- ¹⁶P. Digregorio *et al.* "Full phase diagram of active Brownian disks: From melting to motility-induced phase separation," *Phys. Rev. Lett.* **121**, 098003 (2018).
- ¹⁷J. T. Siebert *et al.* "Critical behavior of active Brownian particles," *Phys. Rev. E* **98**, 030601(R) (2018).
- ¹⁸B. Partridge and C. F. Lee, "Critical motility-induced phase separation belongs to the Ising universality class," *Phys. Rev. Lett.* **123**, 068002 (2019).
- ¹⁹S. Paliwal and M. Dijkstra, "Role of topological defects in the two-stage melting and elastic behavior of active Brownian particles," *Phys. Rev. Research* **2**, 012013(R) (2020).
- ²⁰P. Digregorio *et al.* "Clustering of topological defects in two-dimensional melting of active and passive disks," arXiv:1911.06366.
- ²¹E. Flenner, G. Szamel and L. Berthier, "The nonequilibrium glassy dynamics of self-propelled particles," *Soft Matter*, **12**, 7136 (2016).
- ²²L. Berthier, E. Flenner, and G. Szamel, "Glassy dynamics in dense systems of active particles," *J. Chem. Phys.* **150**, 200901 (2019).
- ²³L. Berthier, E. Flenner and Grzegorz Szamel, "How active forces influence nonequilibrium glass transitions," *New J. Phys.* **19**, 125006 (2017).
- ²⁴N. Klongvess *et al.* "Active glass: Ergodicity breaking dramatically affects response to self-propulsion," *Phys. Rev. Lett.* **123**, 248004 (2019).
- ²⁵J. Stenhammar, R. Wittkowski, D. Marenduzzo, and M. E. Cates, "Activity-induced phase separation and self-assembly in mixtures of active and passive particles," *Phys. Rev. Lett.* **114**, 018301 (2015).
- ²⁶J. Stürmer, M. Seyrich, and H. Stark, "Chemotaxis in a binary mixture of active and passive particles," *J. Chem. Phys.* **150**, 214901 (2019).
- ²⁷S. C. Takatori and J. F. Brady, "A theory for the phase behavior of mixtures of active particles," *Soft Matter*, **11**, 7920 (2015).
- ²⁸A. Kaiser, H. H. Wensink, and H. Löwen, "How to capture active particles," *Phys. Rev. Lett.* **108**, 268307 (2012).
- ²⁹P. M. Vinze, A. Choudhary, and S. Pushpavanam, "Motion of an active particle in a linear concentration gradient," *Phys. Fluids* **33**, 032011 (2021).
- ³⁰R. Ni, M. A. Cohen Stuart, and P. G. Bolhuis, "Tunable long range forces mediated by self-propelled colloidal hard spheres," *Phys. Rev. Lett.* **114**, 018302 (2015).
- ³¹O. Chepizhko and F. Peruani, "Diffusion, subdiffusion, and trapping of active particles in heterogeneous media," *Phys. Rev. Lett.* **111**, 160604 (2013).
- ³²N. Koumakis, A. Lepore, C. Maggi and R. Di Leonardo, "Targeted delivery of colloids by swimming bacteria," *Nature Comm.* **4**, 2588 (2013).
- ³³A. Costanzo, R. Di Leonardo, G. Ruocco and L. Angelani, "Transport of self-propelling bacteria in micro-channel flow," *J. Phys.: Condens. Matter* **24** 065101 (2012).
- ³⁴A. Dhar, P. S. Burada, and G. P. Raja Sekhar, "Hydrodynamics of active particles confined in a periodically tapered channel," *Phys. Fluids* **32**, 102005 (2020).
- ³⁵J. Jiang, B.-Q. Ai, and J.-C. Wu, "Directed Transport of Brownian Particles in a Periodic Channel," *Commun. Theor. Phys.* **64** 320 (2015).
- ³⁶P.-R. Chen, W.-R. Zhong and B.-Q. Ai, "Separation of biological ion in asymmetric nanochannels through alternating electric field," *J. Stat. Mech.* **083203** (2018).
- ³⁷G. S. Redner, A. Baskaran, and M. F. Hagan, "Reentrant phase behavior in active colloids with attraction," *Phys. Rev. E* **88**, 012305 (2013).
- ³⁸F. Y. & Marchetti, M. C. Athermal, "Phase Separation of Self-Propelled Particles with No Alignment," *Phys. Rev. Lett.* **108**, 235702 (2012).
- ³⁹G. S. Redner, M. F. Hagan, and A. Baskaran, "Structure and Dynamics of a Phase-Separating Active Colloidal Fluid," *Phys. Rev. Lett.* **110**, 055701 (2013).
- ⁴⁰J. R. Howse, *et al.* "Self-Motile Colloidal Particles: From Directed Propulsion to Random Walk," *Phys. Rev. Lett.* **99**, 048102 (2007).
- ⁴¹K. Breitsprecher, C. Holm, and S. Kondrat, "Charge me slowly, I am in a hurry: Optimizing charge-discharge cycles in nanoporous supercapacitors," *ACS Nano* **12**, 9733 (2018).

- ⁴²T. M. Mo *et al.* "Ion structure transition enhances charging dynamics in subnanometer pores," ACS Nano **14**, 2395 (2020).
- ⁴³S. Bi *et al.* "Molecular understanding of charge storage and charging dynamics in supercapacitors with MOF electrodes and ionic liquid electrolytes," Nat. Mater. **19**, 552 (2020)
- ⁴⁴E. Locatelli, F. Baldovin, E. Orlandini, and M. Pierno, "Active Brownian particles escaping a channel in single file," Phys. Rev. E **91**, 022109 (2015).
- ⁴⁵S. Kondrat, and A. Kornyshev, "Charging dynamics and optimization of nanoporous supercapacitors," J. Phys. Chem. C **117** 12399 (2013).
- ⁴⁶S. Kondrat, P. Wu, R. Qiao, and A. Kornyshev, "Accelerating charging dynamics in subnanometre pores," Nat. Mater. **13**, 387 (2014).
- ⁴⁷K. Hahn, J. Kärger, and V. Kukla, "Single-file diffusion observation," Phys. Rev. Lett. **76**, 2762 (1996).
- ⁴⁸C. Lutz, M. Kollmann, and C. Bechinger, "Single-File Diffusion of Colloids in One-Dimensional Channels," Phys. Rev. Lett. **93**, 026001 (2004).